Comparison of MEMS accelerometers and geophones at Spring Coulee, Alberta

Michael S. Hons and Robert R. Stewart

ABSTRACT

Geophone and MEMS accelerometer data from a field experiment at Spring Coulee, Alberta are compared in the acceleration domain. At receiver stations where coupling and noise are not a problem, measurements from both sensor types are found to be very similar. Several different analyses of signal-to-noise ratio indicate a small advantage for geophones at low and medium frequencies, at later arrival times and longer offsets. Accelerometers appear to have a small advantage at higher frequencies, shorter arrival times and shorter offsets.

INTRODUCTION

In early January, 2008, a 2D multi-component seismic line was acquired in southern Alberta southwest of Lethbridge. There were two purposes to this survey: first to evaluate the prospectivity of land where the University of Calgary holds mineral rights, and second to do a full side-by-side comparison of Sercel DSU-428 MEMS accelerometers with a state-of-the-art geophone recording system supplied by ARAM Systems Ltd. The full comparison line was processed by other researchers (this volume), but some preliminary results from the raw geophone gathers converted to the acceleration domain are compared to accelerometers here.

There were several different tests within this dataset. The full line was acquired with commercial Vibroseis trucks, recorded into nail-style geophones through the ARAM boxes and also the DSU-428 recorded with Sercel 428XL instruments. There was also a patch of nail-style geophones (CREWES-supplied SM-24s) connected to the Sercel system, so that both the DSUs and the geophones were recorded with the same instrument (channels 169-208, which are labeled 1-40 here). This eliminates any corrections for system response, and provides a very direct comparison of the sensors themselves. In addition to the full program of Vibroseis shots, there were 54 dynamite shots recorded. This analysis will focus on the dynamite shots recorded by the DSUs and the geophones, all connected to the Sercel system. This provides an opportunity to evaluate the largest bandwidth with the least concerns about different field equipment. There were high winds during recording, and some significant noise is expected to show up on the recorded data.

DATA CORRECTION

The geophone traces were corrected to ground acceleration traces using the following transfer function, which is simply a modified version of the more common ground velocity transfer function:

$$\frac{\partial^2 U}{\partial t^2} = \frac{i(\omega_0^2 - \omega^2) - 2\lambda\omega_0\omega}{\omega}\frac{\partial X}{\partial t}, \qquad (1)$$

where U is the displacement of the ground, X is the displacement of the magnet relative to the coil inside the geophone, ω is angular frequency, and λ and ω_0 are the damping coefficient and resonance of the geophone, respectively. Essentially, the recorded geophone trace is ∂X/∂t, and the transfer term operates on it to convert it to ground acceleration ($\partial^2 U/\partial t^2$). This correction provides traces which are very close in appearance, but the scaling of amplitudes between the traces from the two sensors is best determined empirically. In this dataset the best visual fit between amplitude spectra was obtained with a scaling constant of 2.3073 x10^{-2}.

FIELD DATA COMPARISON

The data quality was not always equal between the sensors, which was likely an expression of the coupling conditions at the receiver stations. The 54 dynamite shots into the two stations are shown in a receiver gather for station 2 in Figure 1. At approximately half of the stations the geophone records are less noisy than the DSUs, while in the other half data quality is comparable (e.g. station 17, Figure 2). Observations in the field (Hauer, 2008, pers. comm.) linked some of the noisy DSU stations to inferior plants, with cases not fully inserted into the ground or cables overly exposed to the wind. The very windy conditions likely exacerbated the data quality issue. In the raw records, most of the coherent reflection energy is apparent within the first 2 seconds.

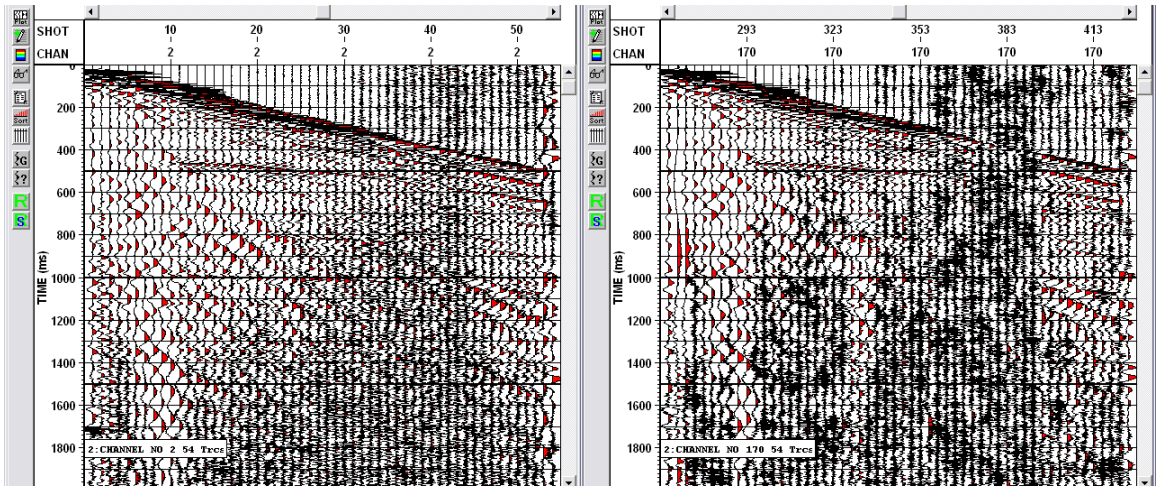

FIG. 1. Comparison of geophone receiver gather (left) at station 2 and accelerometer/DSU (right). A 500 ms AGC and 2 Hz lowcut filter were applied.

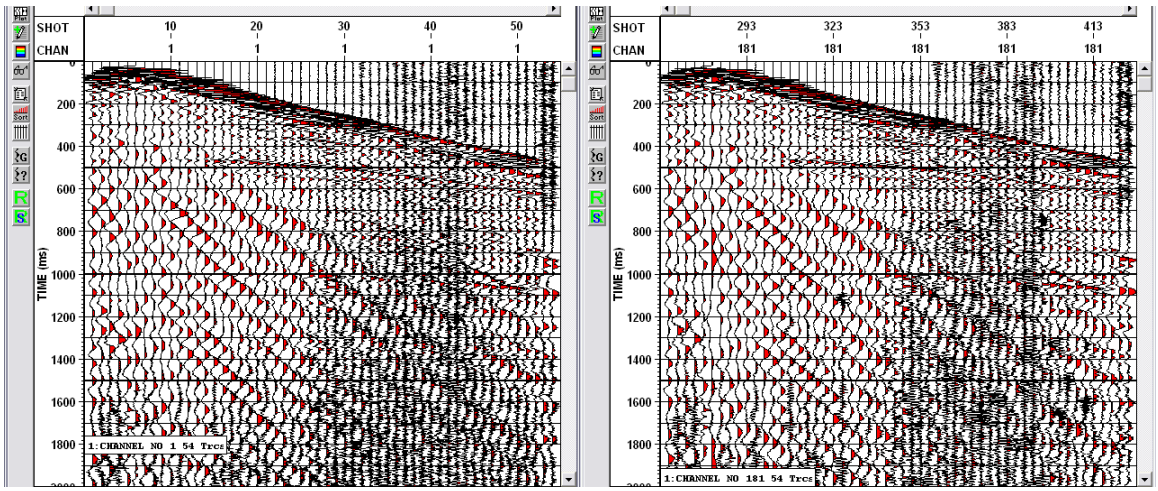

FIG. 2. Comparison of geophone receiver gather (left) at station 17 and accelerometer/DSU (right). A 500 ms AGC and 2 Hz lowcut filter were applied.

Where data quality is fairly good, the simple correction based on the geophone's response results in data traces that are, in general, extremely similar to the accelerometer (Figure 3). Cross-correlation over the full 4 second length of the traces from the two sensors yielded maximum values at or above 97% for traces without noise problems (Figure 4). The average amplitude spectra are very similar as well, both for single stations with comparable data quality (Figure 5) and for the average of all traces recorded by the test patch (Figure 6). The most evident and consistent difference observed in the amplitude spectra is the smaller amplitudes recorded by the geophones at low frequencies (Figure 7). The small amount of difference that does exist may be very important, however, so the rest of the analysis will focus on signal-to-noise ratio to try and determine which sensor acquired more coherent signal.

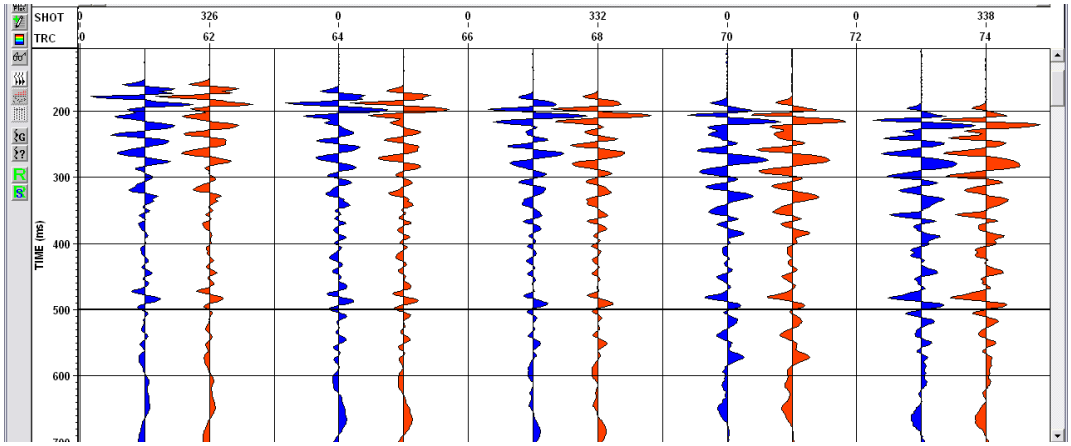

FIG. 3. Comparison of geophone traces corrected to ground acceleration (blue) and DSU accelerometer traces (red).

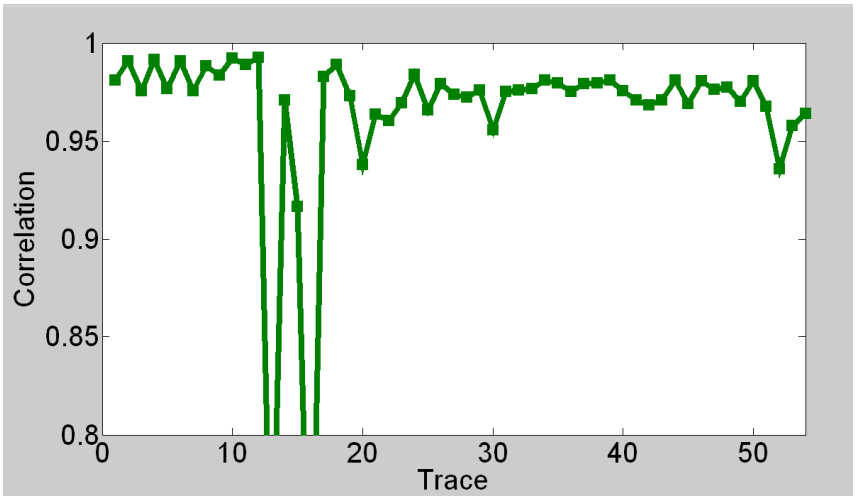

FIG. 4. Cross-correlation of geophone acceleration and DSU traces at station 17.

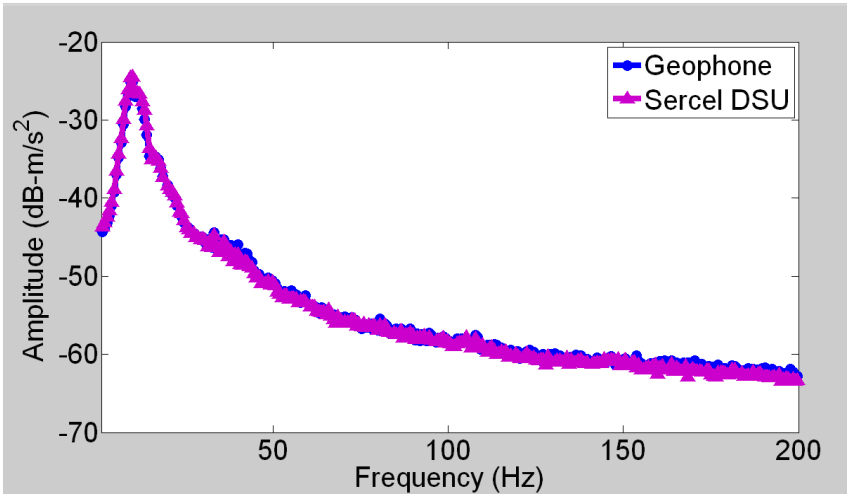

FIG. 5. Average amplitude spectra from station 17, traces 1-54, 500-2000 ms.

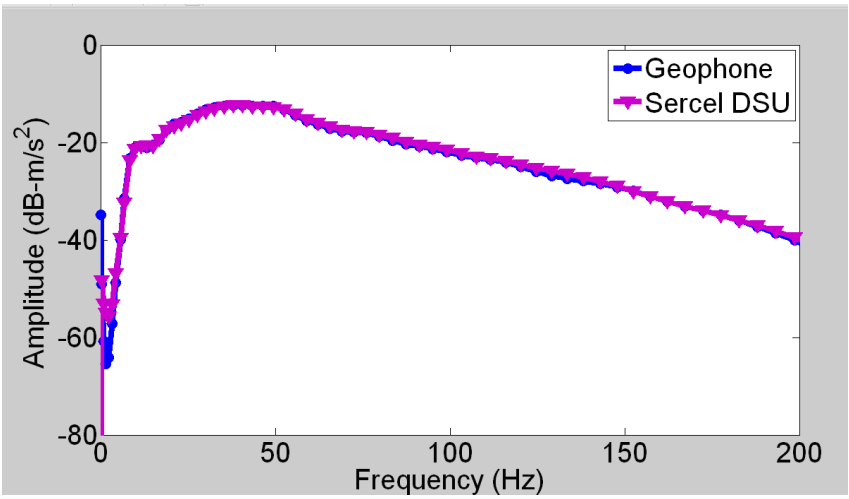

FIG. 6. Average amplitude spectra, all stations, excluding clipped traces.

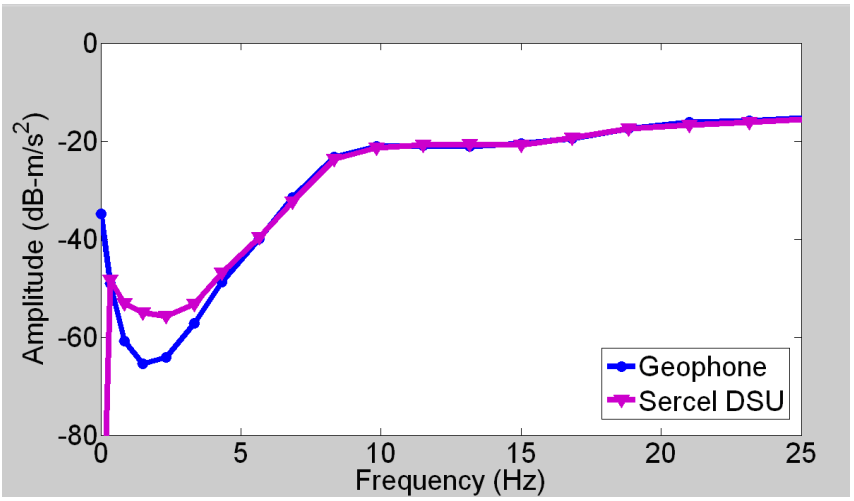

FIG. 7. Closeup of Figure 6, 0-25 Hz.

Examining only the noise before any shot-related signal arrives, we see the observed noise crosses over at ~150 Hz. A crossover is expected because the DSU's sensitivity to acceleration means that its system noise is a relatively smaller contribution at high frequency than for a geophone. This average of all traces likely suffers at the stations with poor plants, however, and looking at one station with comparably data quality, we see the crossover is much lower, around 60-80 Hz.

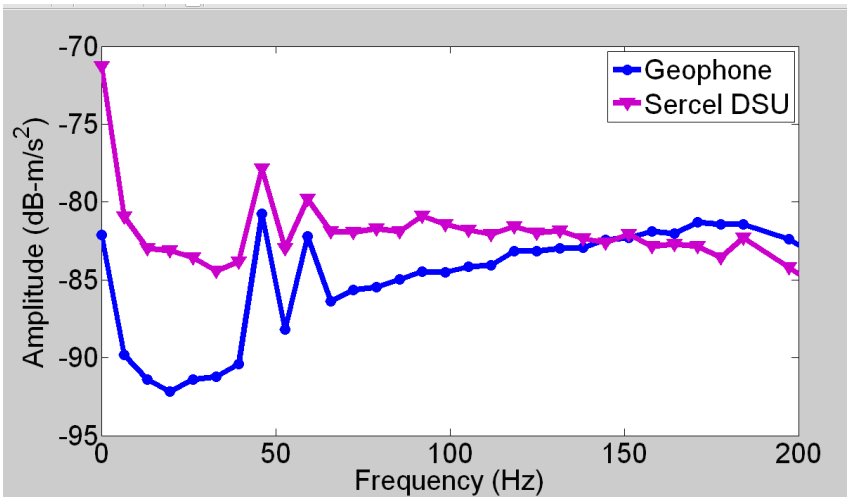

FIG. 8. Average amplitude spectra, all stations, traces 41-54, 0-250 ms.

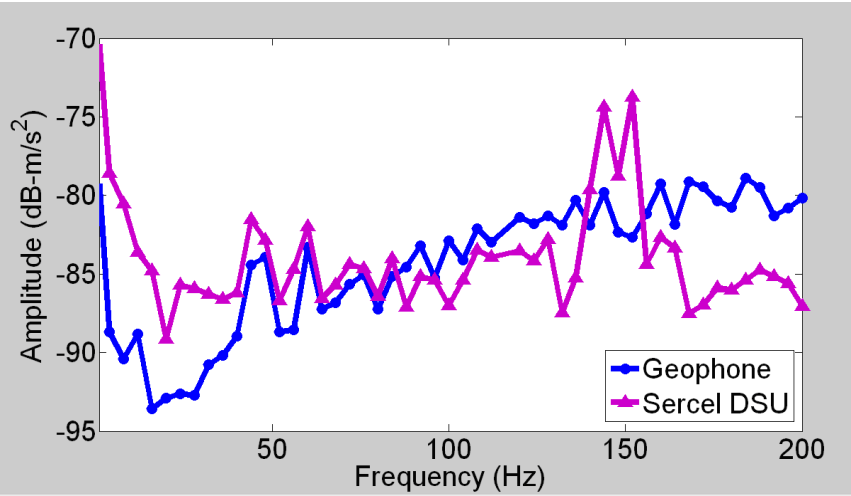

FIG. 9. Average spectra, station 17, traces 40-54, 0-250 ms.

To estimate the S/N for each sensor, the noise before the first break was assumed to be representative of the noise occurring throughout the trace (as long as it was at least 425 ms long), and a 250 ms window beginning just after the first breaks died down was assumed to represent reflection signal with the same noise embedded (traces where a suitable noise record existed tended to have a suitable signal interval free of ground roll). The ratio of the spectra for the two windows yields a S/N estimate, with a DC bias, so the estimated values are not necessarily representative. The results for station 17 are shown in Figure 10, and the average of all stations in shown in Figure 11. The pattern holds true that geophones have a small advantage below 60-80 Hz, and the DSU has a small advantage at higher frequencies. Note that this estimate is based solely on far offset traces.

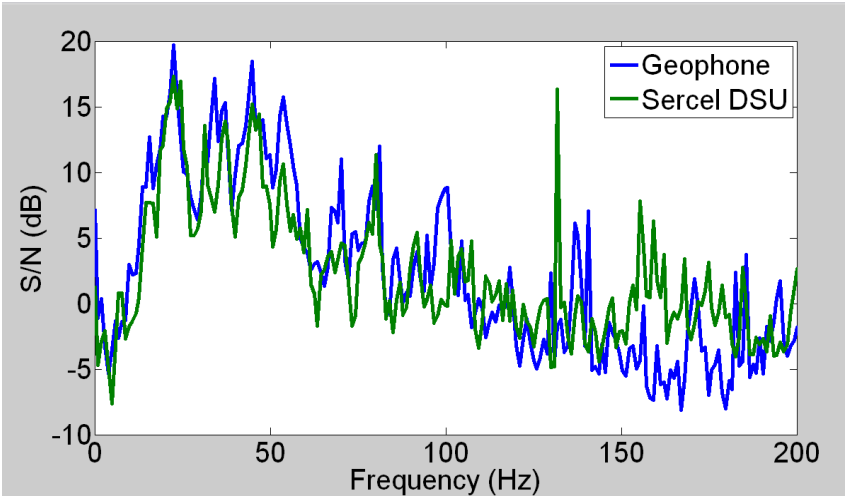

FIG. 10. S/N at station 17, comparing pre-arrival noise to a reflection window.

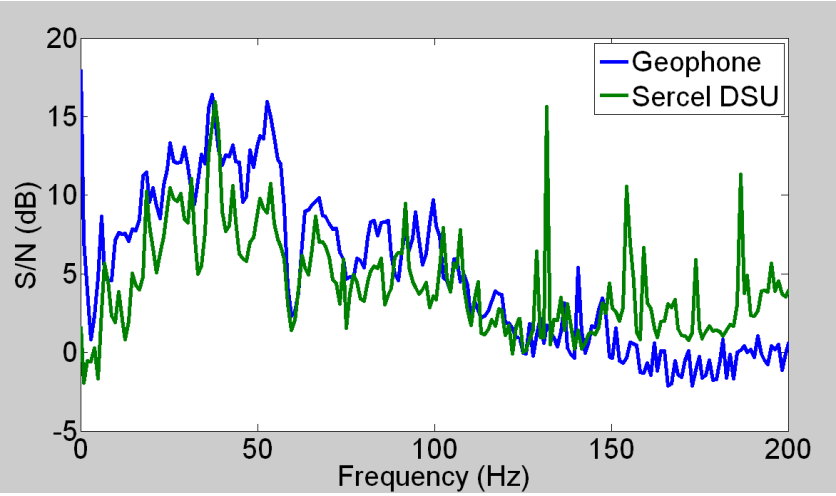

FIG. 11. S/N average of all vertical stations, comparing noise to reflection window.

So far, it appears that the DSUs in the vertical orientation cannot be said to have improved on the low frequency response of the geophones, as their noise appears larger at low frequencies. In an effort to add more weight to this observation, an FX transform was calculated for each sensor at station 17. Interpretation of which FX spectra are more continuous can be an indication of the signal content at each frequency (Margrave, 1999). To the eye it is difficult to spot major differences between the sensors' FX spectra, though it appears that the geophone is somewhat more continuous (Figure 12). Looking closely at the low frequencies, it appears that the extra low frequency amplitude noted in the DSU spectra in Figure 5 is not coherent, and the geophone is moderately more coherent at very low frequencies (Figure 13).

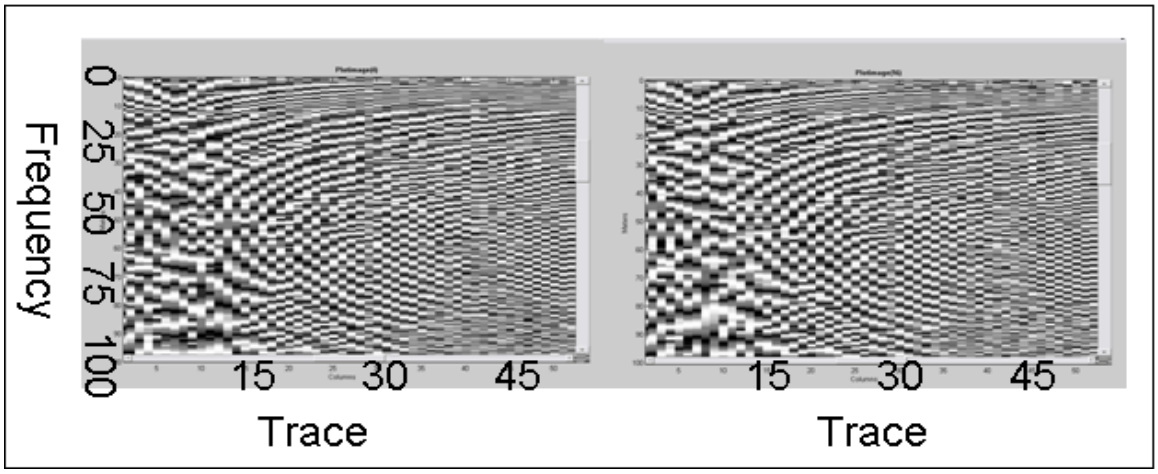

FIG. 12. FX phase coherence at station 17. Left: geophone. Right: DSU.

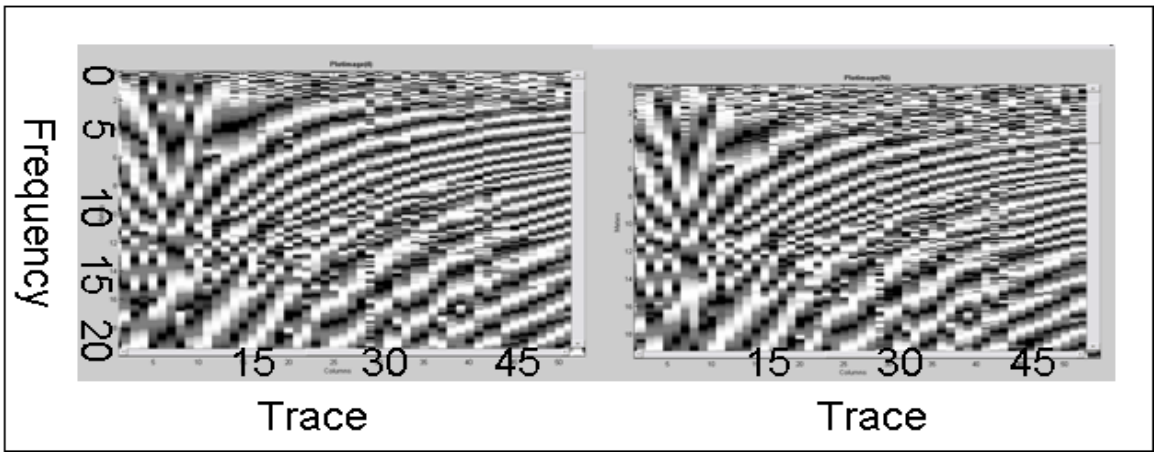

FIG .13. Closeup of Figure 4.13, 0-20 Hz. Left: geophone. Right: DSU.

Finally, within the VISTA processing package is a S/N estimator based on trace-to-trace coherence. To give a reasonable estimate, the data were corrected for elevation statics, and then NMO corrected with the same velocity model. The S/N estimate for station 17 with a sliding window 6 traces wide and 100 ms long is shown for the geophone (Figure 14) and the DSU (Figure 15). While the estimate fails in some areas, and appears to somewhat follow the ground roll, it does a good job of picking out the flattened horizons, especially at shallow depths and longer offsets. A second pattern emerges from this analysis: the geophone has a small S/N advantage at the farthest offsets, consistent with the comparison method before and after first breaks, while the DSU appears to have a small S/N advantage around the strong, shallow arrivals and nearer offsets. This may be a result of the DSU's increased sensitivity to higher frequencies, which will be most apparent in earlier arrivals and smaller offsets. At far offsets, the geophone's lower noise floor around the dominant frequencies becomes dominant, and explains its S/N advantage as offsets increase.

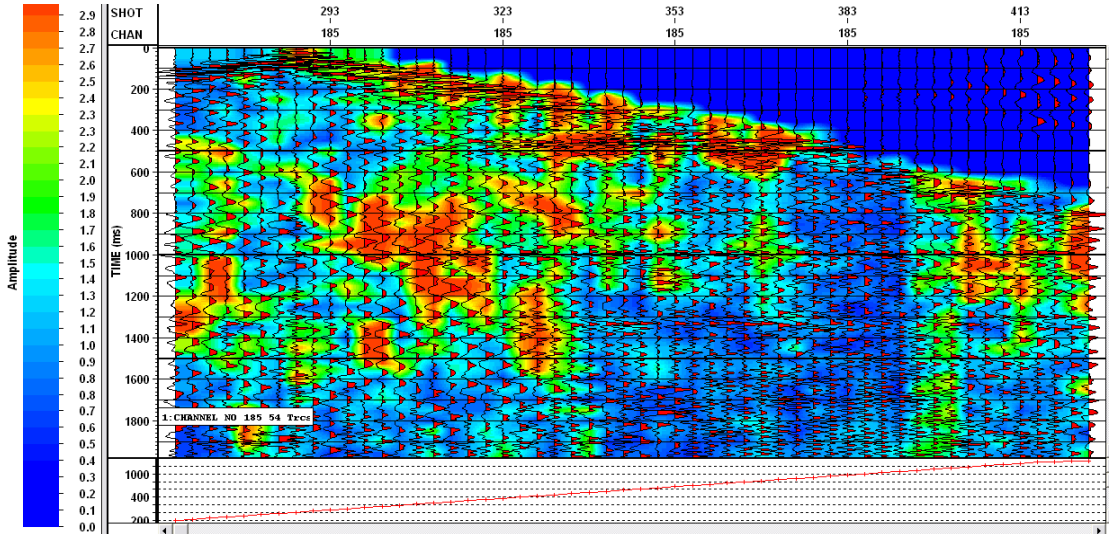

FIG. 14. S/N SM24 chan17-18, overall 1.17.

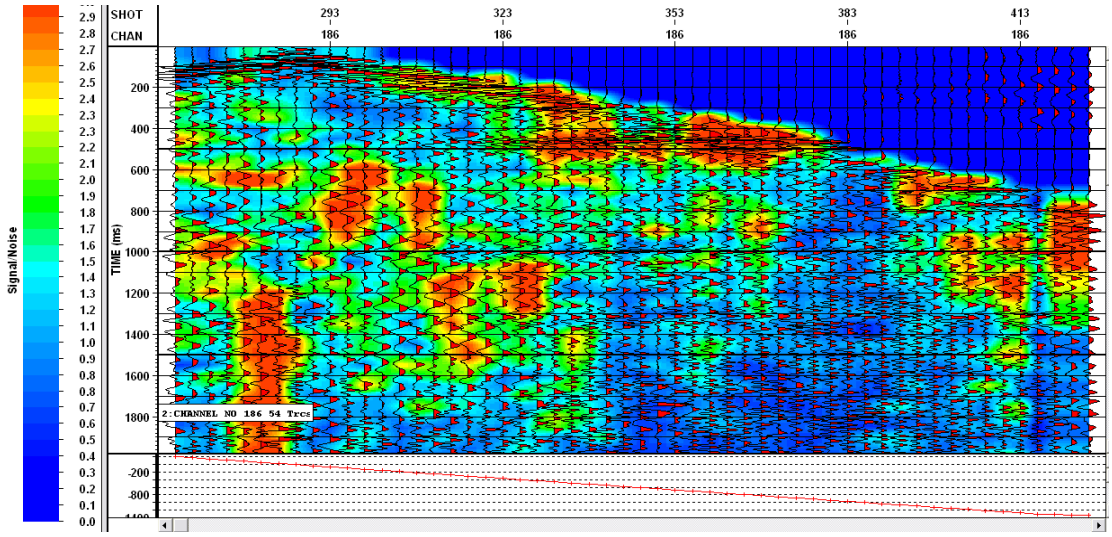

FIG. 15. S/N DSU chan 17-18, overall 1.15

This can be further explored with VISTA's S/N time/frequency analysis tool. Again using a sliding window, this time chosen as 10 traces by 100 ms, the data is examined one band at a time, and the average of the windows at each time sample is output as a S/N trace for each time and each frequency band. The same pattern was apparent is those windows, with the geophone enjoying a S/N advantage at low frequencies and dominant frequencies (Figures 16 and 17), especially at longer arrival times. The DSU appears to remain sensitive to higher frequencies to somewhat longer arrival times (Figure 18), up to ~2.5 seconds, compared with 1.5 seconds for the geophone. This appears to be further confirmation that in the vertical orientation, DSUs have a marginal improvement in sensitivity to high frequencies, and a marginal reduction in sensitivity to low frequencies.

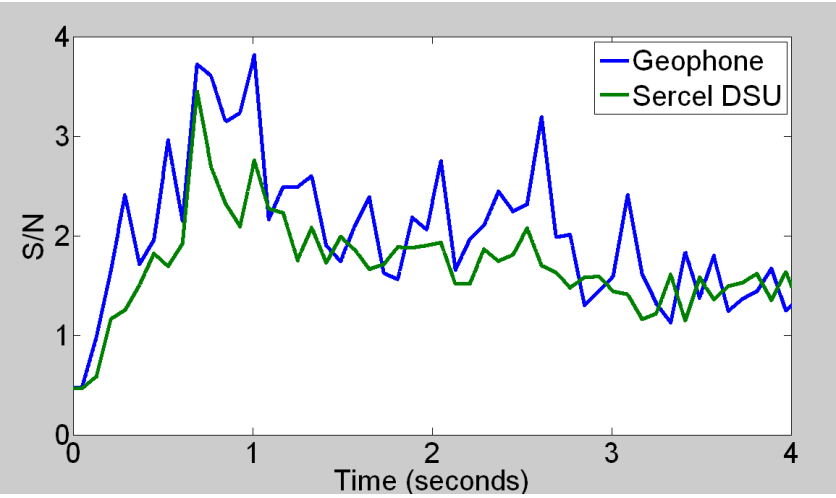

FIG. 16. Time/frequency analysis, frequency band 5-20Hz, 5 Hz rolloff.

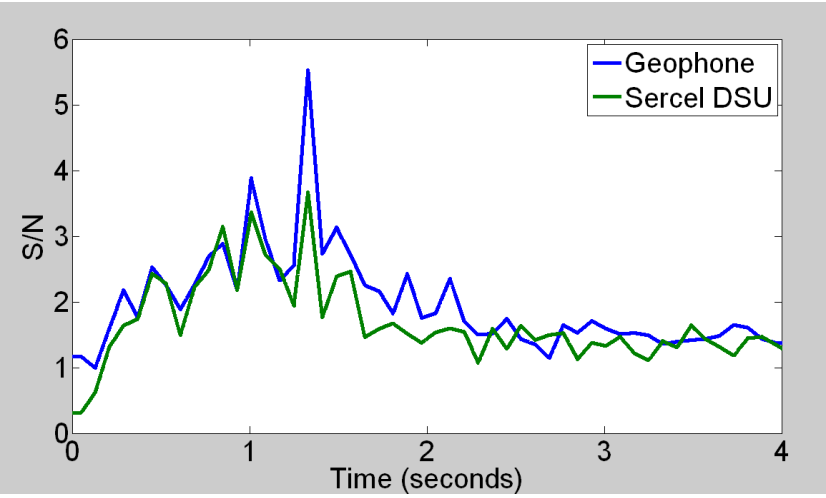

FIG. 17. Time/frequency analysis, frequency band 20-35 Hz, 5 Hz rolloff.

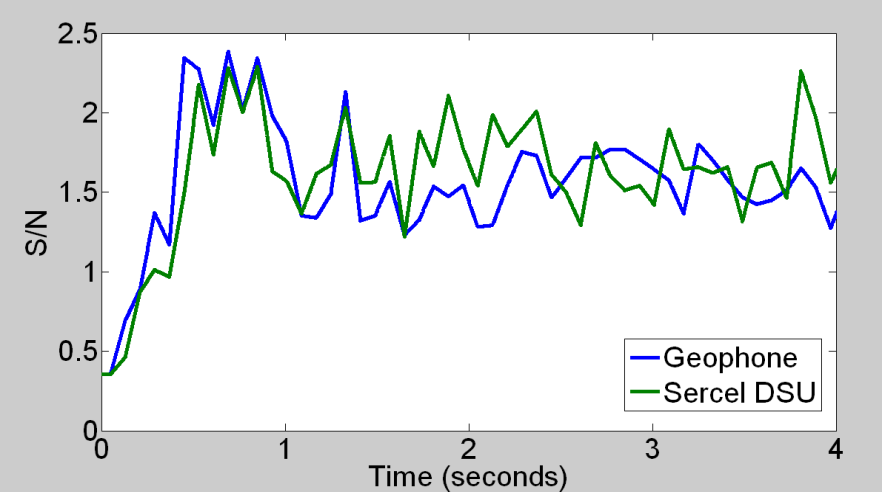

FIG. 18. Time/frequency analysis, frequency band 50-65 Hz, 5 Hz rolloff.

CONCLUSIONS

Geophone data from the Spring Coulee experiment were corrected to ground acceleration traces, for comparison with the recorded accelerometer (DSU) data. Receiver gathers were compared in the time domain and found to be very similar, where data quality was comparable. Some DSU stations suffered from inadequate coupling, exacerbated by extreme wind conditions during recording. Where coupling was adequate for both sensors, traces were very similar, with crosscorrelations over 95%. Examination of the differences in the gathers at a station with similar coupling showed that geophones tended to have higher S/N at frequencies from 5-40 Hz, with indications of improvement at later arrival times and longer offsets. The accelerometers may show a S/N improvement at shorter arrival times and nearer offsets, perhaps due to greater sensitivity to high frequency components in returning signals. No evidence was found for improved recording of low frequencies compared to a geophone, even below 5 Hz. Overall the data from properly coupled sensors is remarkably similar, with observed differences in most of the analyses here being marginal.

REFERENCES

Margrave, G. F., 1999, Seismic signal band estimation by interpretation of f-x spectra: Geophysics, **64**, 251-260.